Original Research Article

Assessment of Aortic Root in Tetrology of Fallot by Multislice Computed Tomography

Abstract

Background: Tetralogy of Fallot (TOF) is the most prevalent cyanotic congenital heart disease (CHD), affecting three out of every 10,000 births. TOF is linked to conal malseptation and lack of rotation, result in failure of the union of the conal and ventricular septa and anterior malalignment of the conal septum, producing the classic tetrad of findings. This work aimed to assess the role of ECG-gated multislice computed tomography (MSCT) in assessing conal malseptation in TOF by measuring the aortic root's clockwise angle rotation, which may serve as a predictor for the degree of conal malseptation and, consequently, the maldevelopment of the right ventricular outflow tract (RVOT).

Methods: This prospective study was performed on 30 individuals who underwent MDCT cardiac angiography of the heart and great vessels. The examined cases were classified into two groups: Group 1 (TOF-PS) TOF with pulmonary stenosis (n=20) and Group 2 (TOF-PA) TOF with pulmonary atresia (n=10). Correlation was done between the rotation angle and main pulmonary artery (MPA) diameter indexed to body surface area.

Results: The TOF-PA group had a larger rotation angle of the root of the aorta compared to TOF-PS group with a statistical significance difference between the two groups ($67.23^0 \pm 13.45^0$ vs $54.34^0 \pm 6.54^0$, P=0.028 respectively). The mean MPA diameter indexed to BSA 12.91 ± 6.05 mm/m^2. The angle of aortic root rotation in a clockwise direction was negatively correlated with the indexed MPA diameter with spearman coefficient = -0.325 and p=0.162. A cut-off value of aortic angle of 56.8°

was determined, above which there is a risk of pulmonary atresia (AUC=0.750, 95% CI= 0.535 – 0.965) with sensitivity 70%, specificity 65%, positive predictive value of was 50% and negative predictive value was 81.2%.

Conclusions: MSCT quantitatively assesses conal malseptation and its impact in individuals with TOF. The aortic root rotates at an angle in the clockwise direction. There is a negative correlation between the degree of aortic root rotation in a clockwise direction and the size of the proximal MPA. Patients diagnosed with TOF with pulmonary atresia (PA) exhibit a greater degree of aortic root rotation.

Keywords: Tetralogy of Fallot, Multislice computed tomography, Aorta, Echocardiography

Introduction:

Tetralogy of Fallot (TOF) is the most prevalent form of cyanotic congenital heart disease (CHD), affecting 3 out of every 10,000 births [1-3]. Sub-pulmonary and pulmonary stenosis, ventricular septal defect (VSD), aortic override, and right ventricular (RV) hypertrophy are the four defining characteristics of the malformation [1, 4, 5].

TOF includes a wide range of anatomical variations, spanning from cases with a VSD with minimal aortic overriding, and mild pulmonary stenosis at one extreme, to those with a severe VSD and pulmonary atresia at the other [1].

It is believed that multiple factors contribute to TOF; trisomy of 21, 18, 13, and microdeletions of chromosome 22q11.2 have been identified among the associated chromosomal abnormalities. [4, 6, 7].

From an embryological perspective, the area where the conus and truncus intersect represents the outflow tract of both ventricles. Resorption as well as differential growth are accountable for reducing conoventricular flange. This reduction leads to the conus moving from the far right approaching the septum's midline to align with the muscular part of the interventricular septum (IVS) [8].

The traditional tetrad of TOF is thought to result from failure of conal and ventricular septal fusion and anterior malalignment of the conal septum, Conal malseptation and a lack of conal rotation are characteristics of TOF .[8, 9].

During embryogenesis, the absence of conal rotation causes the aorta to assume a dextro-position, two potential mechanisms cause aortic root to be displaced to the right: first: possible translation to the right due to the absence of leftward conus migration. Second: rotation clockwise about an eccentric axis, presumed to be secondary to the absence of conal rotation, or a synthesis of these two procedures [3, 9].

The severity of pulmonary (infundibular) stenosis is determined by malseptuation of the conus, which happens at the cost of the pulmonary artery. The blood flow path during embryonic development via pulmonary valves and the aorta is unequal, causing an underdeveloped right ventricle outflow tract (RVOT) [8].

CTA has become indispensable for assessing pediatric CHD. Modern generation of multislice computed tomography (MSCT) enables rapid imaging with enhanced temporal and spatial resolution, greater anatomic coverage per rotation, more consistent enhancement using a smaller volume of intravascular contrast material, and superior 2D reformation and 3D reconstruction [9].

Using ECG-gated MSCT angiography, accurate quantitative evaluations of conal malseptation in TOF patients could be done. The angle of rotation of aortic root in a

clockwise direction may be indicative of conal malseptation severity and, consequently, maldevelopment of RVOT [8].

The purpose of this study was to evaluate the role of ECG-gated MSCT in the evaluation of conal malseptation in TOF by measuring the angle of rotation of the aortic root in the clockwise direction, which may be a potential indicator for the severity of conal malseptation and, consequently, RVOT maldevelopment.

Patients and Methods:

In this prospective study, thirty patients with echocardiographic reports of suspected or confirmed TOF or one of its variants were evaluated for specific anatomic questions raised by inconclusive echocardiography findings, or to confirm the diagnosis before planning appropriate management. The patients underwent MDCT cardiac angiography of the heart and great vessels. They were sent to Tanta University Hospitals radiodiagnosis and medical imaging department by the cardiology and cardio-thoracic departments to undergo MDCT cardiac angiography over the course of a year, from January 2022 to January 2023.

Exclusion criteria were history of allergy to IV contrast media, patients with impaired renal function (creatinine level > 1.5 mg/dl), and patients with bad general condition requiring life support.

Preprocedural preparations:

Patient preparation:

For cases < 5 years (n= 23) chloral hydrate was administered orally to sedate them (n=17) (50–100 mg/kg with a maximum of 2000 mg) or Midazolam given I. V. (n=6) (0.05-0.1mg/kg). Older patients (n=7) were reacting adequately to Words of reassurance and could completely stop breathing. In this study, general anaesthesia was not required. None of the patients were treated with B-blockers to slow HR.

Assessment of the emergency kit includes checking the presence of essential items like an oxygen tank with a mask and extension tube, a blood pressure monitor (sphygmomanometer), and emergency medications like adrenaline for severe low blood pressure or antihistamines for any adverse reactions to contrast agents. Additionally, it should ensure the capability to promptly transfer the patient to the emergency room in case of unmanageable complications.

Technique of CT Examination:

Data acquisition:

A multi-row, 320-slice CT scanner (Aquilion One, Toshiba Medical Systems, Otawara, Japan) was used to scan patients. The position of the patient was supine on the CT table and a chest restrain was applied to minimise motion artifacts. For optimal spatial resolution, the patient's heart was positioned at the isocenter of the gantry. After disinfecting the skin using alcohol, chest wall ECG electrodes were positioned, and continuous monitoring of the ECG trace was performed to confirm the adequacy of the R wave amplitude, which served as the scan trigger. Subsequently, a saline test injection was given to verify proper intravenous access and to check for any leakage once the intravenous line was established. Extravasation of contrast or adverse reactions to contrast medium were to be documented. Afterwards, a scanogram (frontal & lateral views) was obtained, with the scan extending from the neck root, including the proximal common carotid and subclavian arteries, to the portal vein inferiorly. It is of the utmost importance to identify the origin of any possible present MAPCAs, as well as to differentiate co-existing aortic arch branch anomalies, vascular rings, situs abnormalities, and aortic coarctation. Non-ionic and undiluted contrast agent (Ultravist 370, Schering AG, Germany or Omnipaque 350, Nycomed, Amersham) was administered intravenously to 22 and 18 patients,

respectively, using a dual-syringe mechanical power injector (Stellant D, Medrad, Indianola, PA, USA) with a flow rate of 1-1.5 ml/sec increased to 3 ml/sec in older children. The volume of contrast was determined based on body weight (maximum dose of 2 ml/kg). All CT scans were done along the craniocaudal axis using CT parameters that were weight-adjusted. The patients underwent a retrospective ECG-gated CTA volume scan in a single phase. The scanning had 0.35 seconds rotation time and utilized a 80 kV tube voltage . For seven older patients, the tube voltage was adjusted to 100 kV. 15 to 30 minutes after the procedure, the patient was observed until sedation recovery.

Image reconstruction and post processing:

Upon completion of the examination, full volumes were reconstructed in slices with a thickness of 0.5 mm. Multi-slice CT (MSCT) scans were post-processed using a dedicated Vital Images Station (vital images, Vitrea Fx, USA). Malformations of the heart are displayed using maximum intensity projections (MIP), multiplanar (MPR), curved planer reformations (CPR), and three-dimensional volume rendering (VR).

Maximum and minimum intensity projection: peripheral vessels and airways are most effectively viewed as a combination of volume slab sections. CT images are initially obtained at their regular section thickness and subsequently merged in multiples, or "slabs," to produce a thicker composite image using this approach.

Multiplanar reformation (MPR): The reconstruction planes are generated by projecting a line onto one of the cross-sectional slices, aligning the resulting MPR images parallel to the projected line and perpendicular to the cross-sectional plane. For accurate vessel measurements, thin MPR images are utilised.

Curved planar Reformat (CPR): Curved planar images were utilised to visualise vascular structures that curve. It was extremely helpful in evaluating the aorta and major PA.

Volume rendering (VR): acquired after removal of bone. The technique of volume rendering was particularly helpful for displaying structures that run parallel or perpendicular to the transverse plane.

Two visualisation techniques, multiplanar reformation and volume-rendered 3D reconstruction, were used to display the selected images.

The image interpretation was guided by an anatomical and segmental/sequential methodology:

1. Heart: Situs: solitus/ inversus/ ambiguous, atrio-ventricular concordance/ discordance, ventriculo-arterial concordance / discordance, right ventricular outflow assessment (RVOT), interventricular septum: Cono-truncal VSD (type, size), interatrial septum: intact/ ASD (type, size), and morphology of the cardiac chambers.

2. Pulmonary circulation: Pulmonary arteries: Origin, size: Normal/hypoplastic/ atretic, and Proximal MPA diameter was measured on the sagittal plane, the diameter was taken at the widest part before MPA bifurcation during the systole phase. Proximal MPA diameter was indexed for body surface area, PDA, and MAPCAs.

3. Aortic overriding and aortic root rotation.

Perpendicular lines on two orthogonal planes of the aorta were used to identify the short axis of the aortic root on the optimum systolic phase. Any clockwise rotation of the aortic root about its centerline was referred to as an aortic root rotation. Using a true short-axis view of the aortic valve, the aortic root rotation was determined by drawing a line joining the interleafet anterior commissure and the middle of non-coronary sinus then measuring its angle with the interatrial septum plane.

The IAS plane was drawn in the left atrium among anterior and posterior insertion sites for the IAS. (Figure 1)

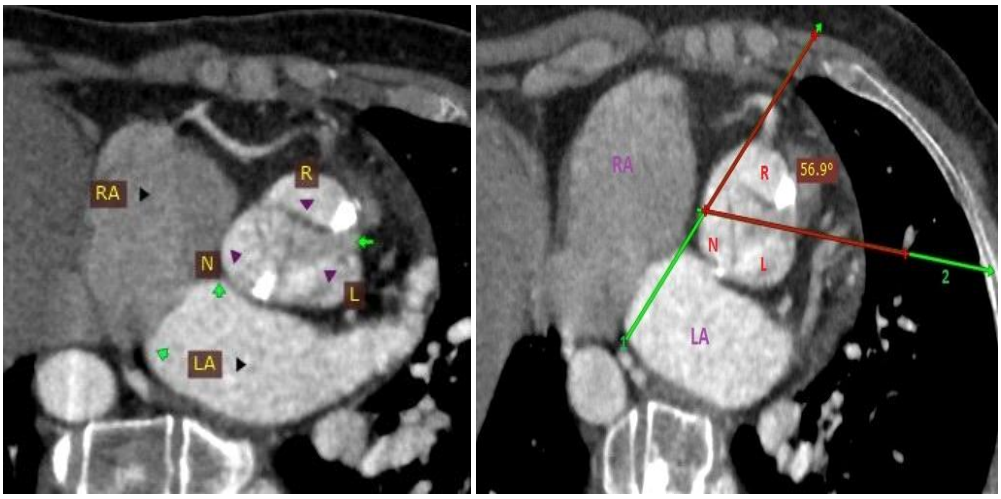

Figure (1): Method for measuring The degree of rotation in the aortic root between the line 1 (the plane of the interatrial septum) and line 2 (connecting the middle of the non-coronary sinus and the anterior commissure) using a true short-axis image of the aortic valve RA, right atrium, LA, left atrium, R right coronary sinus, N, non-coronary sinus, L , left coronary sinus.

Statistical analysis

Data were entered into the computer and analysed using version 20.0 of the IBM SPSS software package. (Armonk, New York: IBM Corporation). Quantitative and percentage descriptions of qualitative information. The Shapiro-Wilk test was utilised to confirm the distribution's normality. The range (minimum and maximum), mean, standard deviation, median, and interquartile range were used to describe quantitative data (IQR). Significance of the obtained results was judged at the 5% level. The used tests were Chi-square test, Monte Carlo correction, McNemar and Marginal Homogeneity Test, Student t-test, Mann Whitney test, Spearman coefficient, and Receiver operating characteristic curve (ROC).

Results:

The cases were subclassified into two groups: **(Group 1)** TOF with pulmonary stenosis TOF-PS (n=20) 66.7 %, who have a forward flow to the pulmonary artery from the RV via a stenotic pulmonary valve. (**Group 2**) TOF with pulmonary atresia TOF-PA (n=10) 33.3%, in cases where there is no forward flow from the right ventricle to the pulmonary arteries, the pulmonary blood supply mainly relies on the patent ductus arteriosus or collateral vessels. The ten cases of the pulmonary atresia with VSD variant were categorized into three types (A, B, and C) based on the condition of the native pulmonary artery (PA), the presence of major aortopulmonary

collaterals (MAPCAs), and the status of the patent ductus arteriosus (PDA). Out of these cases, five (50.0%) belonged to type A, five (50.0%) were classified as type B, and none fell into the category of type C as shown in Table 1.

Table (1): Analysis of the studied individuals according to TOF variant included and PA-VSD types in the study.

	No.	**%**
TOF variant		
TOF PS	20	66.7
TOF PA	**10**	**33.3**
PA-VSD types		
Type 1	5	50.0
Type 2	5	50.0
Type 3	0	0.0

In group 1 (20 cases) there was 13 (65%) males and 7 (35%) females ranging in age from 3 months to 31 years, with median age of 14 months and mean age of 10.48± 16.73 years (125.80 ± 200.80 months) and O2 saturation ranged from 80.0 – 84.0 %, with median O2 saturation of 82% and mean of 81.80 ± 1.61.
In group 2 (10 cases) there was 4 (40%) males and 6 (60%) females, ranging in age from 5 days to 33 years, with mean age of 3.49± 10.36 years (41.99 ± 124.43 months) and O2 saturation ranged from 77.0 – 80.0 %, with median O2 saturation of 78.5% and mean of 78.70 ± 1.06. There was a statistically significant difference between both groups in age, and O2 saturation while there was no difference in gender. (Table 2)

Table (2): Comparison between the two studied groups according to demographic data and O2 sat.

Demographic data	**Group 1 (n = 20)**		**Group 2 (n = 10)**		**p**
	No.	**%**	**No.**	**%**	
Sex					
Male	13	65.0	4	40.0	0.255
Female	7	35.0	6	60.0	
Age (month)					
<6 months	1	5.0	8	80.0	<0.001*
6 m– <1 year	3	15.0	1	10.0	
1 –<2 years	10	50.0	0	0.0	
≥2 years	6	30.0	1	10.0	
Mean ± SD.	125.80 ± 200.80		41.99 ± 124.43		<0.001*

O2 sat			
Mean ± SD.	81.80 ± 1.61	78.70 ± 1.06	<0.001*

IQR: **Inter quartile range** SD: **Standard deviation.**

p: p value for comparing between the studied groups. *: Statistically significant at p ≤ 0.05, Group 1: pulmonary stenosis Group 2: pulmonary atresia

There was a non-statistically significant difference between both MDCT and echocardiography in right ventricular outflow tract obstruction (RVOTO) level detection at the sub-valvular and valvular level, however, both Echocardiography and MDCT exhibited a statistically significant difference in identifying supra-valvular RVOTO with a p-value of less than 0.001, particularly at the level of the main pulmonary artery (MPA) and the left pulmonary artery (PA), where the p-values were 0.001 and 0.039, respectively. However, there was no statistically significant difference between the two methods in the detection of major aortopulmonary collateral arteries (MAPCAs) and PDA detection, but a significant difference in the detection of PDA lesions (P value 0.016). (Table 3)

Table (3): Detection of the level of RV outflow tract obstruction, MAPCAs, and PDA in studied cases by echo and CT.

Level of RVOTO	**Echo (n = 30)**		**CT (n = 30)**		**p**
	No.	**%**	**No.**	**%**	
Sub-valvular	21	70.0	21	70.0	1.000
Valvular PS /PA					
Valvular stenosis	7	23.3	7	23.3	1.000
Valvular atresia	9	30.0	10	33.3	1.000
Supra-valvular (MPA/LPA /RPA) Stenosis, hypoplasia, atresia					
Main pulmonary artery	8	26.7	19	63.3	0.001*
Left pulmonary artery	7	23.3	14	46.7	0.039*
Right pulmonary artery	7	23.3	10	33.3	0.250
MAPCA					
Present	3	10.0	8	26.7	^{McN}**p**=0.063
Absent	27	90.0	22	73.3	
MAPCA number					
1	0	0.0	2	6.7	1.000
2	0	0.0	2	6.7	
3	2	6.7	2	6.7	

more	1	3.3	2	6.7	
MAPCA Lesion					
Present	0	0.0	4	13.3	0.125
Absent	30	100.0	26	86.7	
PDA					
Present	8	26.7	9	30.0	1.000
Absent	22	73.3	21	70.0	
PDA Lesion					
Present	1	3.3	8	26.7	0.016*
Absent	29	96.7	22	73.3	

All cases exhibited a rotation of the aortic root in clockwise direction, with no instances of counterclockwise rotation. The mean aortic root rotation angle of the TOF patients included in the study was $56.63^0 \pm 11.06^0$.
The mean rotation angle of the aortic root in the TOF-PS (Group 1) was $54.34^0 \pm 6.54^0$ and in the TOF-PA (Group 2) was $67.23^0 \pm 13.45^0$. The TOF-PA group had a larger rotation angle of the aortic root compared to TOF-PS group with a statistically significance difference ($67.23^0 \pm 13.45^0$ vs $54.34^0 \pm 6.54^0$, P=0.028 respectively) (Table 4)

Table (4): Comparison between the two studied groups according to angle of the aortic origin rotation

	Total (n= 30)	Group 1 (n = 20)	Group 2 (n = 10)	p
Angle of the aortic origin rotation	$56.63^o \pm 11.06^o$	$54.34^o \pm 6.54^o$	$67.23^o \pm 13.45^o$	0.028*

The mean MPA diameter indexed to BSA in TOF-PS (Group 1) was 12.91 ± 6.05 mm/m2. The indexed MPA diameter showed a negative correlation with the aortic root's clockwise rotation angle with spearman coefficient = -0.325 and p=0.162.

(Figure 2)

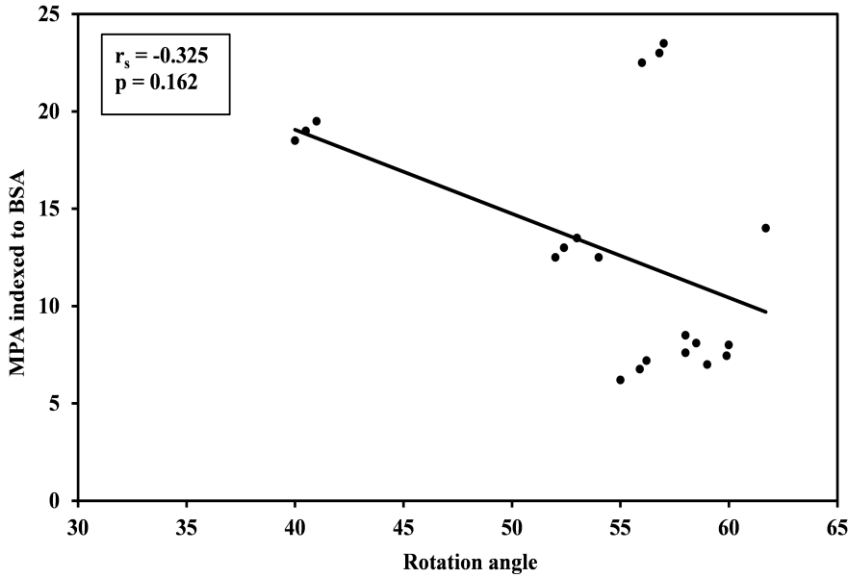

Figure (2): Correlation between rotation angle and MPA diameter indexed to BSA mm/m^2.

A cut-off value of aortic angle of 56.8° was determined, above which there is a risk of pulmonary atresia (AUC=0.750, 95% CI= 0.535 – 0.965) with sensitivity 70%, specificity 65%, positive predictive value was 50% and negative predictive value was 81.2%. (Figure 3)

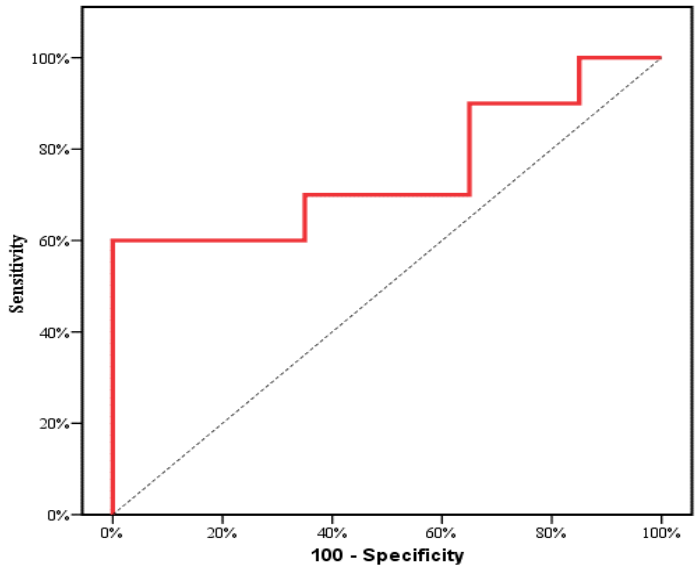

Figure (3): ROC curve for the angle of rotation of the origin of the aortic to predict pulmonary atresia.

MDCT was employed to assess the extent of aortic overriding degree to the interventricular septum, and the results indicated three possible scenarios: equal alignment with both ventricles (50 %), greater alignment(more than 50%) to the left ventricle, or greater alignment (more than 50%)to the right ventricle. Specifically, among the patients, 16 (53.4%) displayed aorta alignment equally to both ventricles, 4 (13.3%) patients exhibited greater alignment to the left ventricle, and 10 (33.3%) patients displayed greater alignment to the right ventricle. In 12 (40.0 %) of the patients, the ascending aorta was dilated.

13(43.3%) patients showed right sided aortic arch and left sided aortic arch found in 17(56.7%) patients.In terms of the aortic arch's branching pattern, MDCT showed that 12 patients had normal branching patterns while the remaining 18 patients had abnormal ones. These abnormal patterns included mirror image branching patterns in nine patients, 6 patients had bovine aortic arches with common origin in the right innominate and left carotid common arteries, while 3 patients had left vertebral arteries origin from aorta. One patient's MDCT revealed aortic coarctation.

By MDCT coronary arteries abnormalities were depicted in 6 (20%) patients, two (6.67%) patients had prominent conus branch, one (3.33%) patient had prominent RV branch, one (3.33%) patient with dual LAD, one arises from RCA and another shorter one from Left main coronary artery, three patients had coronary branch that crosses over RVOT. (Table 5)

Table (5): Distribution of the examined cases based on the degree of aortic overriding, aortic assessment, and coronary anomalies detected by CT.

Degree of aortic overriding detected by CT	**No.**	**%**
Equal (50%) to both ventricles	16	53.4
More to the left ventricle	4	13.3
More to the right ventricle	10	33.3
Aorta assessment by CT	**No.**	**%**
Ascending aorta		
Average	18	60.0
Dilated	12	40.0
Aortic arch side		
Right sided	13	43.3
left Sided	17	56.7
Branching pattern		
Regular	12	40.0
Mirror image	9	30.0
Bovine arch	6	20.0

Vertebral artery from aorta	3	10.0
Coarctation	1	3.3
Coronary arteries anomalies	**No.**	**%**
Sizable conus branch	**2**	**6.67%**
Sizable RV branch	**1**	**3.33%**
Dual LAD	**1**	**3.33%**
Sizable branch crossing over RVOT	**3**	**10%**
Total	**6**	**20%**

Case (1)

14-month girl presented with cyanosis and murmur. (Figure 4, 5)

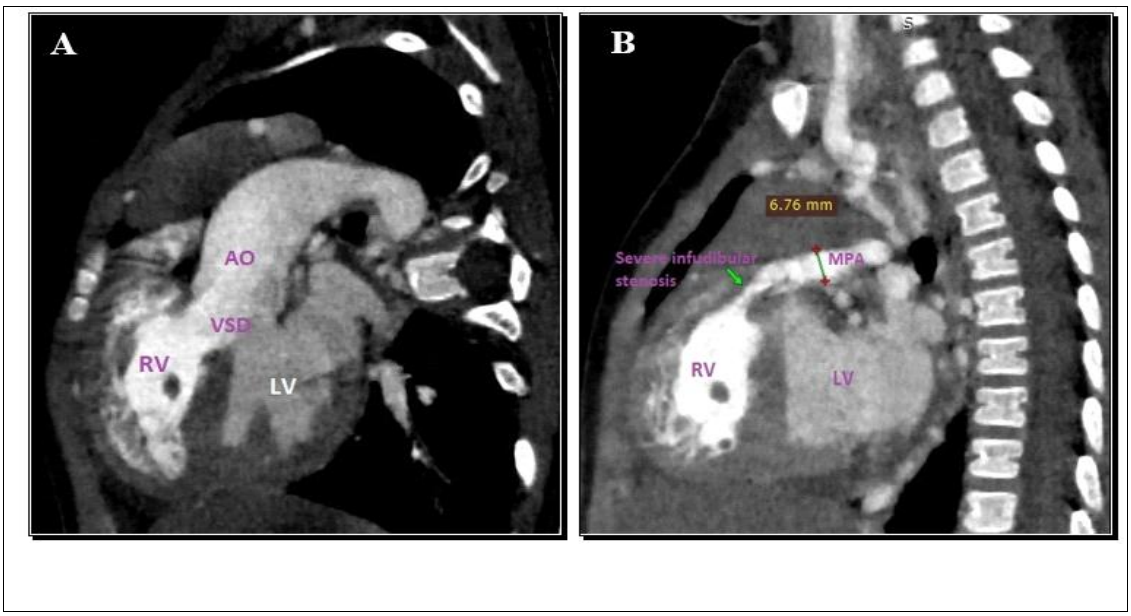

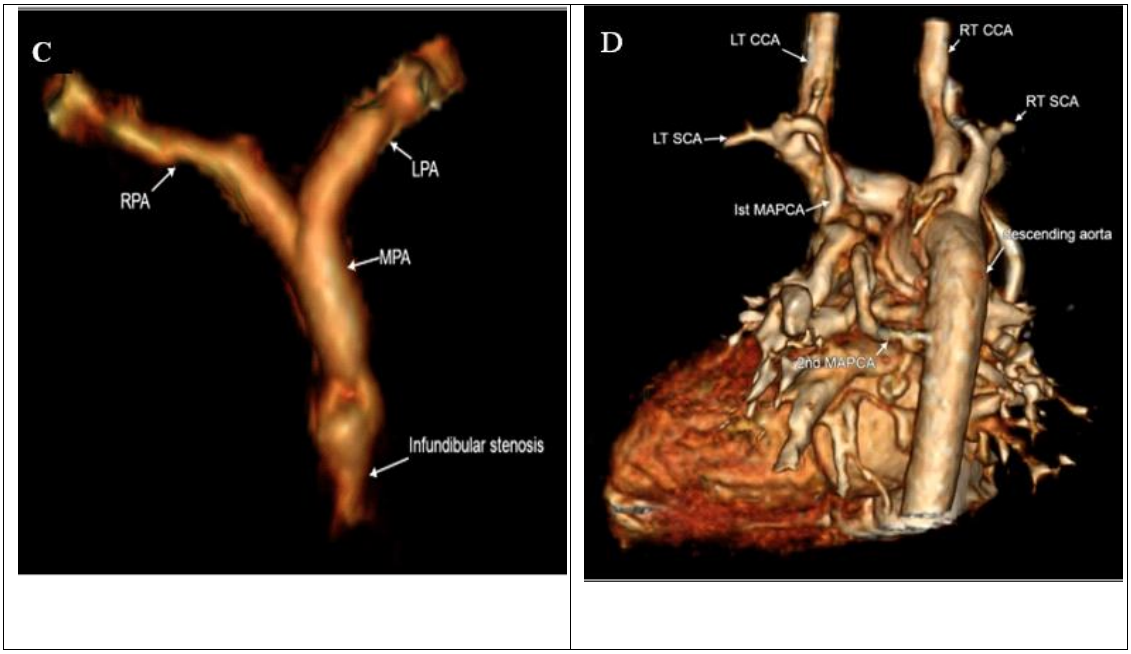

Figure (4): 14 Months old girl with classic TOF (TOF/PS) (A) Oblique reformatted image showing Overriding aorta (50% alignment to each side) with underlying conotruncal ventricular septal defect (VSD) and right ventricular hypertrophy (B) Oblique reformatted sagittal image showing severe infundibular stenosis with hypoplastic MPA (C) 3D VR image showing infundibular stenosis with hypoplastic MPA, RPA & LPA (D) 3d VR image showing MAPCAS

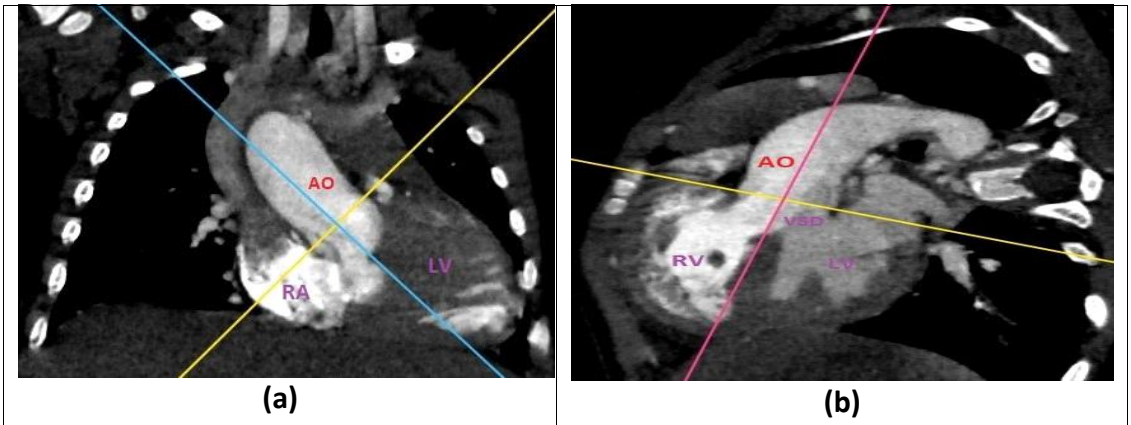

(a) (b)

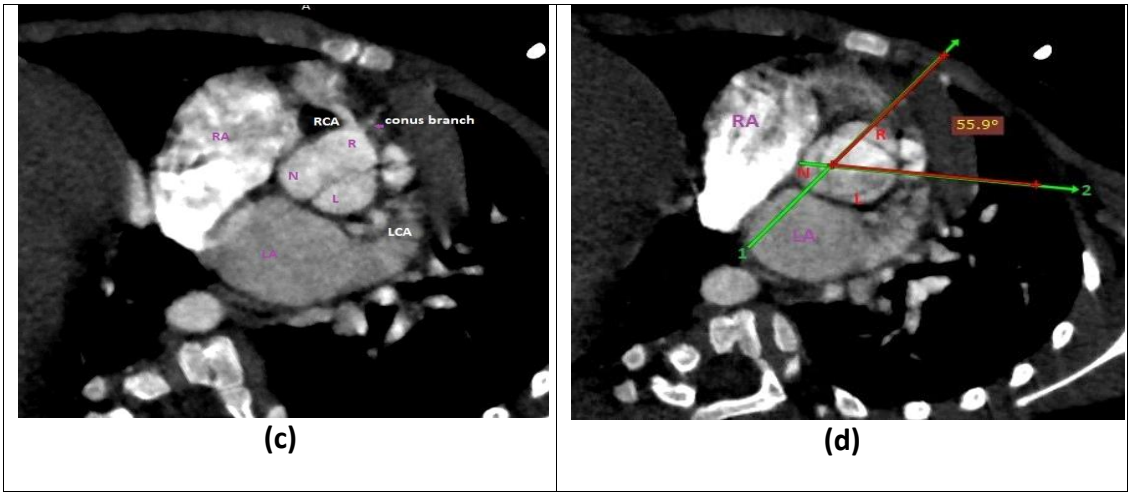

Figure (5): (A) MPR coronal image showing coronal view of aorta, (B) Oblique reformatted image showing sagittal view of aorta, (C) oblique reformatted axial image showing Normal origin of coronary arteries. RCA supplies sizeable conus branch (D) true axial cut of aortic root shows clockwise aortic root rotation with rotation angle 55.9^0

Case (2)

35-day female presented with cyanosis and murmur. (Figure 6,7)

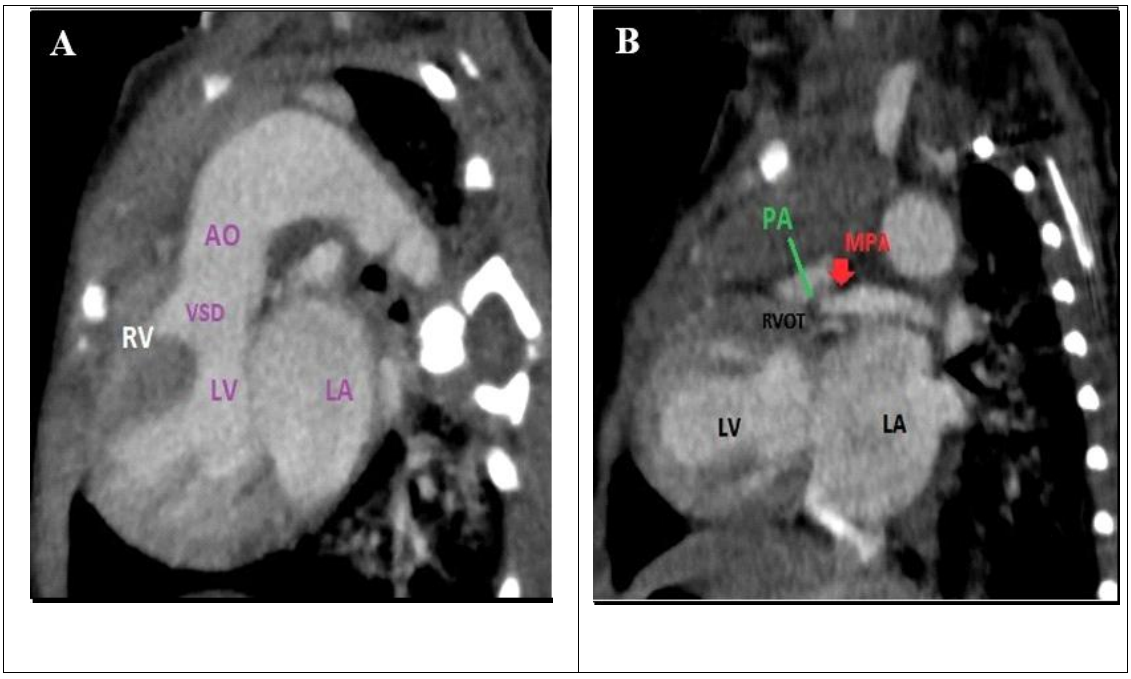

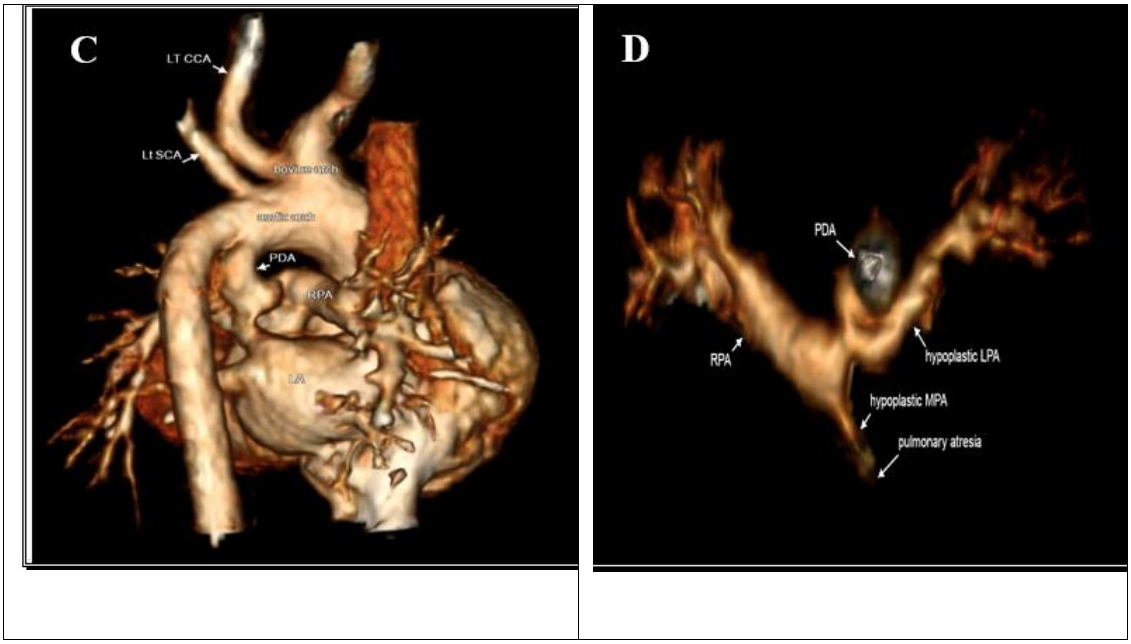

Figure (6): 35 day old female with extreme TOF (TOF/PA) (A) Oblique reformatted image showing Overriding aorta (80% alignment to left side) with underlying conotruncal ventricular septal defect (VSD) and right ventricular hypertophy (B) oblique reformatted sagittal image showing pulmonary atresia (green line) with Small caliber atretic MPA (orange arrow) (C)VR image showing bovine arch and PDA to LPA (D) VR image showing hypoplastic MPA with sizable RPA and hypoplastic LPA

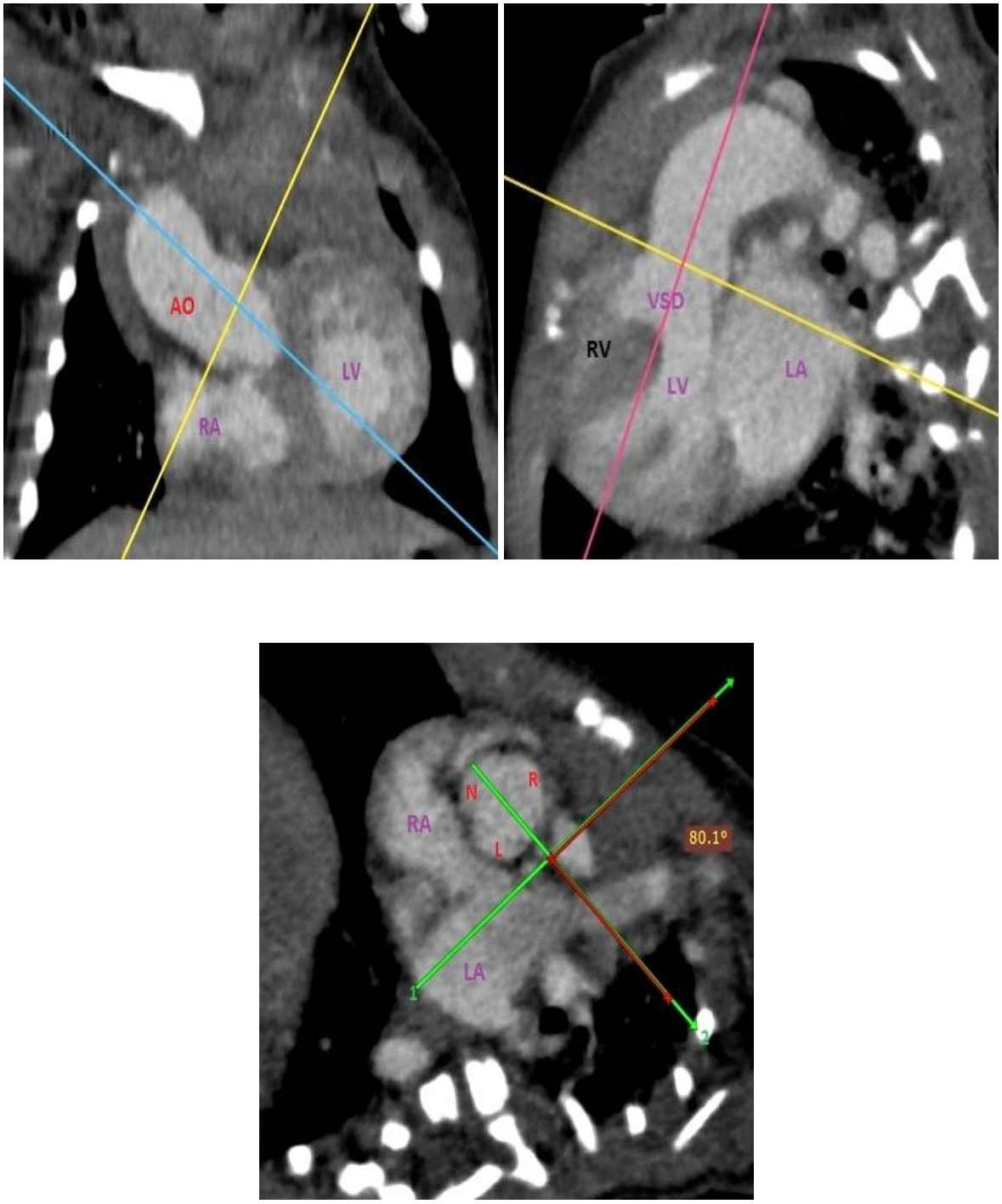

Figure (7): (D) MPR coronal image showing coronal view of aorta, (E) Oblique reformatted image showing sagittal view of aorta, (F) true axial cut of aortic root shows clockwise aortic root rotation with rotation angle 80.1^{0}

Discussion

In this study, we evaluate the utility of ECG-gated MSCT in the evaluation of conal malseptation in TOF by measuring the aortic root's clockwise angle rotation, which

may serve as a predictor for the degree of conal malseptation and, consequently, the maldevelopment of the RVOT.

We classified the 30 examined cases into TOF with pulmonary stenosis (TOF /PS) including 20 patients, and TOF with pulmonary atresia (PA/VSD) including 10 patients. the ten cases of PA with VSD (PA – VSD) variant were further subclassified into three types based on the presence or absence of pulmonary arteries of origin, MAPCAs, and patent PDA (A, B and C). There were five cases of type A, five cases of type B, and none of type C.

This is consistent with Romeih et al [8] who classified the TOF patients to two group but with much larger sample size, 91% of patients have TOF with pulmonary stenosis TOF-PS group with age ranging from 2 months–40 years, and mean age of 2 years and O_2 saturation of 72±5% and 29 patients (9%) have TOF with pulmonary atresia (TOF-PA) with age ranged from 1 month to 33 years, and mean age of 5 years and O_2 saturation of 71±7%.

Situs solitus was observed in every case in our study; no abnormal situs was identified. Our outcomes are consistent with Zakaria et al. [10] who reported TOF patients with an abnormal situs are uncommon.

In our study, MDCT detected the four classic TOF symptoms in 100 percent of cases which corresponds with Shehata et al. [11] and Moustafa et al. [12] in their research.

In each case, the level of obstruction of the right ventricular outlet tract is evaluated; infundibular (sub-valvular) PS was the most affected level which was evident in 21 (70%) patients. This was in line with the findings of Hrusca et al. [13], who used non-ECG-

gated CT angiography to examine pulmonary artery anomalies in tetralogy of Fallot a

nd discovered that twenty-four patients had infundibular stenosis. Also, Singh et al. [14] and Moustafa et al. [12] reported that their patients were most affected by infundibular stenosis.

In our study there was 100% agreement between MDCT and Echocardiography in the detection of sub-valvular stenosis, there is no statistically significant difference between MDCT and Echocardiography in the detection of valvular level of RVOTO, however, Echocardiography missed diagnosis of valve atresia in one patient.

On the other hand, in detecting supra-valvular stenosis, there was a statistically significant difference between the two modalities with p-value <0.001, at the MPA and left pulmonary artery levels with p values of 0.001 and 0.039, respectively. These results aligned with Hu et al. [15] whose MDCT detection of supra-valvular pulmonary stenosis was 100 % accurate when compared to cardiac catheterization.

MPA stenosis/obstruction was observed in 19 individuals, which accounts for 63.3% of the patients, followed by LPA stenosis in 14 patients (46.7%), and RPA stenosis in 10 patients (33.3%). These findings align with the results reported by Moustafa et al. [12] and Zakaria et al. [10], who stated that the most prevalent pulmonary artery abnormality was combined MPA stenosis and its branches with 17 % incidence. This contrasts with the findings of Sheikh et al. [16], the most frequent anomaly reported by 10% of their patients was isolated left pulmonary stenosis. Discrepancy is attributable to the greater sample size in the study by Moustafa et al. [12], which included approximately 5000 patients who underwent cardiac catheterization.

In this study, MSCT identified nine patients with patent ductus arteriosus (PDA), whereas echocardiography identified eight patients. Furthermore, CT successfully detected a tightly narrowed pulmonary end of PDA in three patients and a stenosed or occluded aortic end in two patients, which echocardiography failed to do. These

findings are consistent with the results reported by Moustafa et al. [12] and Shehata et al. [17]. Ishihara et al. [18] also recommended the use of MSCT for better evaluation in cases where PDA is suspected despite a normal echocardiogram. However, Leschka et al. [18] favored transthoracic echocardiography (TTE) as the primary method for PDA diagnosis, with MDCT playing a limited role.

MSCT detected 22 MAPCAs per 8 patients (26.7%). Echocardiography detected only seven MAPCAs per three patients. In addition to assessing the origin, number, size, and course of MAPCA-supplied lung segments, CT detected stenosis in the MAPCA in four patients, which concurred with Hu et al. [15] who stated CT has a superior role in assessing the number, origin, and supply of MAPCA lung lobes irrespective of their size, whereas TTE is only able to recognize the largest. Chandrashekhar et al. [19] found MDCT had the same function as catheterization for identify collaterals of aortopulmonary, whereas echocardiography's small field of view makes it difficult to detect these collaterals.

Our study verified that the aortic root rotates in clockwise direction in patients with TOF. all the TOF patients we evaluated showed a clockwise rotation of the aortic root; there were no instances of a counterclockwise rotation. Our findings revealed that TOF-PA has a much greater aortic root rotation angle than TOF with PS, the mean rotation angle was $54.34^{o} \pm 6.54^{o}$ VS $67.23^{o} \pm 13.45^{o}$ in TOF-PS and TOF-PA respectively. the aortic root clockwise rotation angle has a negative correlation with the indexed MPA diameter ($r = -0.325$). Our study proposed a cut-off aortic angle of 56.8°, beyond which individuals with TOF are more prone to having a pulmonary valve that is atretic rather than stenotic.

These results aligned with those of Romeih et al. [8] who stated that all studied TOF patients exhibited aortic root clockwise rotation, average rotation angle in TOF PA

being significantly greater than that of TOF PS, (with P=0.001). Romeih et al. [8] also reported that negative correlation among the clockwise rotation angle of the aortic root and the indexed MPA diameter. Also, a cut-off aortic angle of 58.4°, beyond which the risk of pulmonary atresia is elevated.

Our findings support the morphological research performed by Burggren et al. [20] and Goenezen et al. [21] that presented the geometric characteristics of conal malseptation in TOF. Results by Goenezen et al. [21] and Erhardt et al. [22] found alterations in inflow patterns could potentially impact the migration of neural crest cells and the production of cellular fibronectin, a glycoprotein found in the extracellular matrix that is essential for the development of cardiac and other tissues. These changes may contribute to subsequent issues with conus underdevelopment.

Six patients (20 percent) were found to have coronary artery abnormalities in our study. These findings similar to Elshimy et al. [23], Hrusca et al. [13] who reported anomalies of coronary artery incidence (20 % and 22.85% respectively). However, this disagrees with Sheikh et al. [16] who detected coronary artery anomalies in 4.9 % of cases, and Shehata et al. [11] who reported coronary artery irregularities in 3.3% of cases.

Our research showed, 16 (53.4%) had equal aortic alignment to both ventricles, 10 (33.3%) had more than 50% alignment to the right ventricle in the TOF/DORV variant, and 4 (13.3%) had more than 50% alignment to the left ventricle. Our finding were in keeping with Moustafa et al. [12] who reported that The most common condition, reported in 78% of patients, was equal aortic overriding, which was followed by more alignment to the RV in 19.5% of patients and more alignment to the LV in only 2.6% of patients and with Shehata et al. [11] who reported that aortic

overriding alignment more to the RV (DORV type) found in 9 (30%) while equal alignment and more to LV alignment were found in 21 (70%) patients collectively.

MDCT detected normal branching pattern in 12 (40%) patients while abnormal branching pattern was detected in 18 (60%) patients, this was similar to Tawfik et al. [24] results which reported pattern of normal branching in TOF patients 36 percent, 9 (30%) patients had a mirror image branching pattern. Additionally, one patient was diagnosed with aortic coarctation using MDCT.

Among the limitations of the study are limited sample size, Because of that, the suggested cut-off rotation angle of the aortic root, beyond which individuals with TOF are more prone to having a pulmonary valve that is atretic rather than stenotic, exhibited moderate sensitivity and specificity. This aspect might be validated by additional multicenter research.The relationship between the proposed cut-off aortic root rotation angle and the prognosis of TOF patients is an area that requires further multicenter research.

Conclusions:

MSCT quantitatively assesses conal malseptation and its impact in individuals with TOF. The aortic root rotates at an angle in the clockwise direction. There is a negative correlation between the degree of aortic root rotation in a clockwise direction and the size of the proximal MPA. Patients diagnosed with TOF with pulmonary atresia (PA) exhibit a greater degree of aortic root rotation.

References:

1. Bedair R, Iriart X. EDUCATIONAL SERIES IN CONGENITAL HEART DISEASE: Tetralogy of Fallot: diagnosis to long-term follow-up. Echo Res Pract. 2019;6:R9-r23.

2. Domnina YA, Kerstein J, Johnson J, Sharma MS, Kazmerski TM, Chrysostomou C, et al. Tetralogy of Fallot. Critical Care of Children with Heart Disease: Basic Medical and Surgical Concepts. 2020:191-7.

3. Bozok S, Kestelli M, Ilhan G, Gokalp O, Ozpak B, Akyuz M, et al. Tips and pearls for "true" dextroposition of the aorta in tetralogy of Fallot. Cardiol Young. 2013;23:377-80.

4. Bamigboye-Taiwo OT, Adeyefa B, Onakpoya UU, Ojo OO, Eyekpegha JO, Oguns A, et al. Tetralogy of Fallot in the nascent open-heart surgical era in a tertiary hospital in south-west Nigeria: lessons learnt. Cardiovasc J Afr. 2022;33:122-6.

5. van der Ven JP, van den Bosch E, Bogers AJ, Helbing WA. Current outcomes and treatment of tetralogy of Fallot. F1000Research. 2019;8.

6. Kalyan S, Das S, Raj V. Pre-and Postoperative Imaging in Tetralogy of Fallot. CT and MRI in Congenital Heart Diseases. 2021:315-30.

7. Jernigan EG, Strassle PD, Stebbins RC, Meyer RE, Nelson JS. Effect of Concomitant Birth Defects and Genetic Anomalies on Infant Mortality in Tetralogy of Fallot. Birth Defects Res. 2017;109:1154-65.

8. Romeih S, Kaoud A, Hashem M, Abdelfattah M, Gibreel M, Elzoghby M, et al. A quantitative assessment of aorta root rotation in patients with tetralogy of Fallot evaluated by MSCT. Sci Rep. 2021;11:14336.

9. Wong PC, Miller-Hance WC. Transesophageal Echocardiography for Pediatric and Congenital Heart Disease: Springer Nature; 2021.

10. Zakaria RH, Barsoum NR, Asaad RE, El-Basmy AA, Azab AO. Tetralogy of Fallot: imaging of common and uncommon associations by multidetector CT. The Egyptian Journal of Radiology and Nuclear Medicine. 2011;42:289-95.

11. Shehata SM, Zidan EH, Hasan BA, Mohi TM. Preoperative assessment of tetralogy of Fallot variants and associated anomalies by MDCT cardiac angiography. Zagazig University Medical Journal. 2022;28:1485-93.
12. Moustafa SAEF, Hussein MM, Sultan AA, Bilal MMZ, El Gamal MAF, Sobh DM. Three steps approach for preoperative evaluation of tetralogy of Fallot patients: role of 128 MDCT. Egyptian Journal of Radiology and Nuclear Medicine. 2021;52:1-14.
13. Hrusca A, Rachisan AL, Gach P, Pico H, Sorensen C, Bonello B, et al. Detection of pulmonary and coronary artery anomalies in tetralogy of Fallot using non-ECG-gated CT angiography. Diagn Interv Imaging. 2016;97:543-8.
14. Singh RKR, Jain N, Kumar S, Garg N. Multi-detector computed tomography angiographic evaluation of right ventricular outflow tract obstruction and other associated cardiovascular anomalies in tetralogy of Fallot patients. Pol J Radiol. 2019;84:e511-e6.
15. Hu BY, Shi K, Deng YP, Diao KY, Xu HY, Li R, et al. Assessment of tetralogy of Fallot-associated congenital extracardiac vascular anomalies in pediatric patients using low-dose dual-source computed tomography. BMC Cardiovasc Disord. 2017;17:285.
16. Sheikh AM, Kazmi U, Syed NH. Variations of pulmonary arteries and other associated defects in Tetralogy of Fallot. Springerplus. 2014;3:1-4.
17. Shehata S, Zaiton F, Warda MA, Shahbah D, Ebrahim B. Value of MDCT as a non-invasive modality in evaluation of pediatric congenital cardiovascular anomalies. The Egyptian Journal of Radiology and Nuclear Medicine. 2017;48:467-78.

18. Ishihara A, Funabashi N, Ozawa K, Takaoka H, Kobayashi Y. The use of whole thoracic ECG-gated MDCT for the de novo diagnosis of isolated patent ductus arteriosus in middle aged or older subjects. Int J Cardiol. 2016;224:62-4.
19. Chandrashekhar G, Sodhi KS, Saxena AK, Rohit MK, Khandelwal N. Correlation of 64 row MDCT, echocardiography and cardiac catheterization angiography in assessment of pulmonary arterial anatomy in children with cyanotic congenital heart disease. Eur J Radiol. 2012;81:4211-7.
20. Burggren W, Filogonio R, Wang T. Cardiovascular shunting in vertebrates: a practical integration of competing hypotheses. Biol Rev Camb Philos Soc. 2020;95:449-71.
21. Goenezen S, Rennie MY, Rugonyi S. Biomechanics of early cardiac development. Biomech Model Mechanobiol. 2012;11:1187-204.
22. Erhardt S, Zheng M, Zhao X, Le TP, Findley TO, Wang J. The Cardiac Neural Crest Cells in Heart Development and Congenital Heart Defects. J Cardiovasc Dev Dis. 2021;8.
23. Elshimy A, Khattab RT, Hassan HGEMA. The role of MDCT in the assessment of cardiac and extra-cardiac vascular defects among Egyptian children with tetralogy of Fallot and its surgical implementation. Egyptian Journal of Radiology and Nuclear Medicine. 2021;52:1-9.
24. Tawfik AM, Sobh DM, Ashamallah GA, Batouty NM. Prevalence and types of aortic arch variants and anomalies in congenital heart diseases. Academic Radiology. 2019;26:930-6.